Expression of organic anion-transporting polypeptides 1B1 and 1B3 in ovarian cancer cells: relevance for paclitaxel transport

Svoboda, M ; Wlcek, K ; Taferner, B ; Hering, S ; Stieger, B ; Tong, D ; Zeillinger, R ; Thalhammer, T ; Jäger, W

Abstract: Our results revealed OATP1B1 and OATP1B3 as high-affinity paclitaxel transporters expressed in ovarian cancer cell lines and tumor tissues, suggesting a role for these polypeptides in the disposition of paclitaxel during therapy.

DOI: https://doi.org/10.1016/j.biopha.2011.04.031

Expression of organic anion-transporting polypeptides 1B1 and 1B3 in ovarian cancer cells: relevance for paclitaxel transport

Martin Svoboda[a], Katrin Wlcek[b], Barbara Taferner[c], Steffen Hering[c], Bruno Stieger[d], Dan Tong[e], Robert Zeillinger[e], Theresia Thalhammer[a], Walter Jäger[b,*]

[a]*Department of Pathophysiology, Medical University of Vienna, A-1090 Vienna, Austria*

[b]*Department of Clinical Pharmacy and Diagnostics, University of Vienna, A-1090 Vienna, Austria*

[c]*Department of Pharmacology and Toxicology, University of Vienna, A-1090 Vienna, Austria*

[d]*Division of Clinical Pharmacology and Toxicology, University Hospital Zurich, CH 8091 Zurich, Switzerland*

[e]*Molecular Oncology Group, Department of Obstetrics and Gynecology, Medical University of Vienna, A-1090 Vienna, Austria*

*Corresponding author: Tel.: +43-1-4277-55576. Fax: +43-1-4277-9555. E-mail: walter.jaeger@univie.ac.at

Abstract

Purpose: Ovarian cancer remains a deadly malignancy because most patients develop recurrent disease that is resistant to chemotherapy. Organic anion-transporting polypeptides (OATPs) mediate the uptake of clinically important drugs thereby effecting intracellular drug accumulation. In this study, we investigated whether OATPs may also contribute to paclitaxel transport in estrogen-responsive and estrogen-independent ovarian carcinoma cell lines and tumor tissue.

Methods: Expression of all 11 human OATPs in human ovarian cancer tissue samples and in the ovarian carcinoma cell lines OVCAR-3 and SK-OV-3 was investigated using real-time RT-PCR. Kinetic analysis of paclitaxel uptake was characterized in both cell lines and in OATP-transfected *Xenopus laevis* oocytes. Cytotoxicity of paclitaxel in OVCAR-3, SK-OV-3 and OATP1B1- and OATP1B3-transfected SK-OV-3 cells was performed using the CellTiter-Glo assay.

Results: OATP1B1 and OATP1B3 are active paclitaxel transporters in transfected *X. laevis* oocytes. Real-time RT-PCR analysis revealed expression of both OATPs in human ovarian cancer tissue specimens and in cancer cell lines. The higher mRNA levels for OATP1B1 and OATP1B3 found in SK-OV-3 cells correlated with higher initial uptake rates for paclitaxel. In addition, cytotoxicity studies with OATP1B1- and OATP1B3-transfected SK-OV-3 cells demonstrated lower IC_{50} values compared to cells transfected with the empty vector.

Conclusions: Our results revealed OATP1B1 and OATP1B3 as high-affinity paclitaxel transporters expressed in ovarian cancer cell lines and tumor tissues, suggesting a role for these polypeptides in the disposition of paclitaxel during therapy.

Keywords: ovarian cancer, paclitaxel, OATPs, PCR, SK-OV-3, OVCAR-3

1. Introduction

Ovarian cancer is often diagnosed at an advanced stage because early symptoms are inconspicuous and reliable diagnostic biomarkers are not available [1]. This contributes to a poor 5-year overall survival rate of < 40% and a high death rate [2]. A combination of paclitaxel together with platinum derivatives is applied in standard chemotherapy after initial surgery on the tumor [3]. Although high response rates to this initial regimen are observed, a relapse is seen in two-thirds of patients. This is due to the rapid development of drug resistance, which is often caused by a reduced accumulation of the drug in cancer cells [4,5].

It is well established that overexpression of ATP-powered efflux pumps such as P-glycoprotein (P-gp) or MDR1, encoded by the *ABCB1* gene, induce drug resistance to cytotoxic agents including paclitaxel [6]. Indeed, taxane resistance due to overexpression of P-glycoprotein (MDR1) has been shown in ovarian cancer [7]. Overexpression of the multidrug resistance-related proteins MRP2 (*ABCC2*), MRP3 (*ABCC3*) and MRP7 (*ABCC10*) have been identified as paclitaxel-resistance factors in various cell lines and tumor tissues including HER-2-amplified breast carcinoma and non-small-cell lung cancer [8-10]. However, uptake mechanisms into tumor cells might be even more important than efflux transporters for the efficacy of anticancer drugs because they are determinants for intracellular drug concentration [11].

One of the most important cellular drug uptake mechanisms in humans is via members of the organic anion-transporting polypeptide family (OATP) [12,13]. Official nomenclature differentiates between genes and protein, using the terms "*SLCO*" and "OATP," respectively [14]. To facilitate readability and understanding of this manuscript, "OATP" is used for both genes and proteins. OATPs are expressed in a variety of tissues [15] and tumors [16,17], where they mediate the transport of endogenous and exogenous compounds, including drugs [12,13,18]. Studies have shown that uptake

transporters can confer sensitivity to anticancer agents [19-23], such as the OATP1B3 substrate methotrexate [19]. This may be therapeutically important because expression of OATP varies greatly among tumor cell lines [24}.

Cellular uptake of paclitaxel is known to be facilitated by OATP1B3 in X*enopus laevis* oocytes [25] and by Oatp1a/1b in mice, strongly affecting plasma levels and tissue distribution of paclitaxel [28]. Furthermore, it was shown that paclitaxel is also transported by the organic anion transporter 2 (OAT2; gene: *SLC22A7*) [26] expressed in humans, predominantly in the liver and kidney [27]. It is unknown whether OAT2 is also expressed in human cancer cells. As OATPs exhibit overlapping substrate specificity, we hypothesized that additional OATPs may also contribute to the uptake of paclitaxel. To gain further insight into the possible role of OATP transporters in the chemoresistance of ovarian cancer, we characterized the OATP mRNA expression profiles in estrogen-responsive OVCAR-3 [29] and the estrogen-independent SK-OV-3 [30] ovarian cancer cell lines, and we investigated paclitaxel transport in *X. laevis* oocytes expressing all human OATPs. Our results demonstrate that paclitaxel uptake in OATP1B1 and OATP1B3 correlated with OATP1 and OATP3 mRNA expression, indicating a role for these transporters in tumor therapy.

2. Material and methods

2.1. Materials

[^{3}H]paclitaxel (740 GBq/mmol) was purchased from American Radiolabeled Chemicals (St. Louis, MO). The ovarian carcinoma cell lines OVCAR-3 and SK-OV-3 were originally obtained from the ATCC (Manassas, VA). Fetal Calf Serum (FCS) was obtained from Invitrogen (Carlsbad, CA). The ovarian carcinoma cell lines were maintained in phenol-red free RPMI-1640 medium supplemented with L-glutamine

(PAN-Biotech GmbH, Aidenbach, Germany), 10% FCS and 1% penicillin (10.000 U/ml) / streptomycin (10 mg/ml) solution (Invitrogen) in a humidified atmosphere at 37 °C with 5% CO_2.

2.2. Patient samples

Frozen samples were obtained from patients undergoing routine surgery at the Department of Obstetrics and Gynecology, Medical University of Vienna. Informed consent was obtained from all patients, and permission for the study was obtained from the ethical committee of the institution. Pathological inspection revealed that all tumors were serous epithelial carcinomas. Patient characteristics, tumor staging and grading [31] are summarized in Table 1. Total RNA from healthy ovary tissue was obtained from Stratagene (La Jolla, CA).

2.3. TaqMan® real-time RT-PCR

Total RNA from OVCAR-3 and SK-OV-3 cancer cells and human ovarian cancer tissues was isolated using the RNeasy® Mini kit (Qiagen, Hilden, Germany), and the RNA was treated with RNase-free DNase (Qiagen) to remove genomic DNA. The concentration, purity and integrity of the RNA samples were determined using a Nanodrop ND-1000 (Kisker-Biotech, Steinfurt, Germany) and agarose gel electrophoresis. 1 μg of total RNA was reverse-transcribed in 20-μl reactions using the High-Capacity cDNA RT kit (Applied Biosystems, Foster City, CA) with the provided random hexamer primers and RNase inhibitor (Applied Biosystems) according to the manufacturer's instructions. TaqMan® Gene Expression Assays (Applied Biosystems) were purchased for all eleven human OATPs and four transporters from the ABC family (Table 2). Control assays for the *ACTB* (PN 4326315E) and *HPRT1* (PN 4310890E) genes were also purchased from Applied Biosystems. Prefabricated primers and probes for the endogenous control

genes *GAPDH* and *RPL13A* were obtained from PrimerDesign (PrimerDesign Ltd., Southampton, UK). TaqMan® real-time RT-PCR was performed in an amplification mixture volume of 10 µl containing 5 µl 2x TaqMan® Gene Expression PCR Master Mix (Applied Biosystems), 0.5 µl of the appropriate Gene Expression Assay, 10 ng template cDNA diluted in 4 µl nuclease-free water and 0.5 µl nuclease-free water. Thermal cycling conditions were 2 min at 50 °C and 10 min a t 95 °C, followed by 40 cycles of 15 s at 95 °C and 1 min at 60 °C on the 7900HT Sequenc e Detection System (Applied Biosystems) equipped with a 96-well fast cycling block. The results were imported into DataAssist™ 2.0 software (Applied Biosystems) for automated data analysis using the comparative Ct (ΔΔCt) method [32]. A normalization factor (NF) was calculated by averaging the Ct values of the four endogenous control genes *ACTB*, *GAPDH*, *HPRT* and *RPL13A* via the geometric mean. Relative quantities (RQ) for every sample were then calculated by the formula $RQ = 2^{(-\Delta Ct) / 2(-\Delta Ct_{reference})}$, where ΔCt = Average Ct – NF. The standard deviation (SD) was calculated for Ct values of the technical replicates and was used to calculate the RQ_{Min} and RQ_{Max}:

$RQ_{Min} = 2^{(-\Delta Ct - SD) / 2(-\Delta Ct_{reference})}$

$RQ_{Max} = 2^{(-\Delta Ct + SD) / 2(-\Delta Ct_{reference})}$

according to the DataAssist™ v2.0 Software User Instructions (Applied Biosystems).

2.4. Immunohistochemistry

Immunohistochemistry staining experiments were done on 4-µM paraffin sections from ovarian cancer samples. Before application of antibodies, antigen retrieval was performed for 2 minutes in citrate buffer using a microwave oven (R-208, Sharp Electronics Europe, Vienna, Austria). Dilutions for primary antibodies were 1:100 for OATP1B1/1B3 (#BM5541, Acris, Herford, Germany), and incubations lasted for 16 hrs at 4°C, while the incubation with species-specific peroxidase-labeled IgG lasted for 1

hour. Thereafter, sections were processed for DAB visualization using the Envision+ System-HRP (DAB) kit (Dako, Glostrup, DK). Slides were mounted in Mowiol 4-88 (Carl Roth, Karlsruhe, Germany), and the OATP staining pattern was observed using an Axioplan 2 microscope (Carl Zeiss AG, Oberkochen, GE).

2.5. Transient expression of OATP1B1 and OATP1B3 in SK-OV-3 cells

OATP1B1 and *OATP1B3* cDNA sequences (Kullak-Ublick et al. 2001) were inserted into the multiple cloning site of pCMV6-XL4, and the nucleotide sequence of the coding regions were confirmed by nucleic acid sequencing (MWG, Ebersberg, Germany). Exponential growth-phase SK-OV-3 cells were reverse transfected using FuGENE® HD Transfection Reagent (Roche, Basel, CH) at a lipid/DNA ratio of 3:1 (6 µl/2 µg). Briefly, 2 µg of DNA was diluted into 100 µl of Opti-MEM (Invitrogen), 6 µl of FuGENE reagent was added, mixed and incubated for 15 min at room temperature. Subsequently, the transfection complex was transferred to one well of a six-well plate, and SK-OV-3 cells were added at 4 x 10^5 per well in 2 ml of RPMI-1640 medium supplemented with 10% FCS (without antibiotics). Based on low transfection efficiency, OATP1B1- and OATP1B3-transfected OVCAR-3 cells were not included in any further experiments.

2.6. Cytotoxicity assay

A total of 1000 cells/well (OVCAR-3, SK-OV-3, OATP1B1-transfected SK-OV-3 and OATP1B3-transfected SK-OV-3) were seeded in 96-well plates. After 48 h, cells were treated with graded concentrations of paclitaxel (0.5, 1.0, 2.0, 4.0, 6.0, 10.0 and 50.0 nM) or 0.1% solvent dimethyl sulfoxide as control. Cell viability was measured after 48 h using the CellTiter-Glo® Assay (Promega, Madison, WI) and a Victor™ microplate reader (PerkinElmer, Waltham, MA). Corresponding IC_{50} values were calculated by non-linear regression analysis using GraphPad Prism 5 software (GraphPad, La Jolla, CA).

2.7. Preparation of OATP cDNA for the expression in X. laevis oocytes

The plasmids containing human full-length cDNA from OATP1B1 (pSPORT1) and OATP1B3 (pSPORT1) were originally cloned from a human liver cDNA library, and OATP2B1 (pCMV6-XL4) was cloned from a human brain cDNA library [33]. OATP1A2 (pDRIVE, IHS1382-8428120), OATP2A1 (pOTB7, EHS1001-6793541) and OATP4C1 (pENTR223.1, OHS4559-99620240) full-length cDNA clones were purchased from Open Biosystems (Thermo Fisher Scientific, Huntsville, AL). The lacking stop codon in the OATP4C1 clone was reconstructed by PCR using 0.5 mM dNTPs, 12.5 pmol of each primer, 0.5 U Hot Start Phusion® DNA polymerase (Finnzymes, Espoo, FI) and 1x HF buffer (Finnzymes) in a final volume of 25 µl. The following primer sequences were used (start codon in bold): forward: 5'-CC ACC **ATG** AAG AGC GC-3' and reverse: 5'-TCA CCC TTC TTT TAC TAT TTT GTT G-3'. Thermal cycling conditions were 98 °C for 30 s, followed by 25 cycles of 98 °C for 10 s, 62 ° C for 20 s and 72 °C for 1 min on a MyCycler™ (Bio-Rad, Hercules, CA). The obtained full-length OATP4C1 PCR fragment was subcloned into the pJET1.2 vector (Fermentas, St.Leon-Rot, Germany) using blunt-end cloning with a CloneJET PCR cloning kit (Fermentas) according to the manufacturer's instructions. OATP1C1 (pBluescriptR, IRAKp961I0832Q) and OATP4A1 (pOTB7, IRALp962P0734Q) plasmids were purchased from Imagenes (Berlin, Germany). To obtain full-length cDNA sequences of OATP3A1 and OATP5A1, we purchased total RNA from normal human ovaries (MVP™, Stratagene, La Jolla, CA). Total testis RNA (Clontech Laboratories, Inc., Mountain View, CA) for the cloning of OATP6A1 was kindly donated by Dr. D. Mechtcheriakova (Department of Pathophysiology, Medical University of Vienna, Austria). Reverse transcription was performed by preincubation of 0.4 µg total RNA with 0.5 µg oligo(dT) primers in a volume of 11 µl for 5 min at 65 °C. Subsequently, 9 µl of reverse transcription master mix was added, containing 0.5 mM of dNTPs (Fermentas), 20 U of RNaseOUT™

(Invitrogen, Carlsbad, CA), 200 U of RevertAid™ H Minus M-MuLV reverse transcriptase (Fermentas) and 1x reaction buffer in a final volume of 20 µl. The mixture was incubated at 45 °C for 1 h followed by 70 °C for 10 min. The sequence of OATP6A1 was amplified from 50 ng of testis cDNA, and the sequence of OATP3A1 and OATP5A1 from 50 ng of ovary cDNA; the rest of the amplification cocktail consisted of 0.5 mM of dNTPs, 12.5 pmol of each primer, 0.75 µl DMSO, 0.5 U Hot Start Phusion® DNA polymerase (Finnzymes, Espoo, FI) and 1x GC buffer (Finnzymes) in a final volume of 25 µl. Primer sequences were the following (start codons are in bold): OATP3A1, forward: 5'-A AGG **ATG** CAG GGG AAG AAG C-3', reverse: 5'-GCC CTC CTT TAG TCA CTA TAA AAC GG-3'; OATP5A1, forward: 5'-TGA ATT CTA AGC GCC **ATG** GAC GAA-3', reverse: 5'-TCT TCC ATT TTC AAG CTT CAG GAG G-3'; and OATP6A1, forward: 5'-A GCC **ATG** TTC GTA GGC GTC GC-3', reverse: 5'- ATC ACA ATG ATG ATC CAG TTA CAA GTC AG-3'. PCR conditions for OATP3A1 were 98 °C for 30 s, followed by 40 cycles of 98 °C for 10 s, annealing at 68.5 °C for 20 s and extension at 72 °C for 1 min on a Bio-Rad MyCycler™. The conditions for OATP5A1 and OATP6A1 were identical except for annealing at 66 °C. The purified cDNA was then cloned into the pJET1.2 vector using the CloneJET PCR cloning kit (Fermentas). Sequences of OATP3A1, OATP5A1 and OATP6A1 were checked by forward and reverse full-length sequencing (MWG) and compared to the appropriate reference sequences (OATP3A1 transcript variant 1: NM_013272.3; OATP5A1: NM_030958.1; OATP6A1: NM_173488.3). In OATP3A1, we found a polymorphism for 1083G>C, resulting in the amino acid exchange of Glu294Asp. For OATP5A1, we detected an SNP at 1406C>G, leading to the amino acid exchange of Leu264Val. No polymorphisms were found in OATP6A1.

2.8. Linearization, template preparation, and in vitro transcription of OATP cRNA

All plasmid inserts were verified for correct sequence and orientation by sequencing (MWG). For the *in vitro* synthesis of cRNA, the cDNA clone of OATP4A1 was linearized with BglII, and MluI was used for the linearization of OATP1B1 and OATP1B3 plasmids. For OATP3A1, OATP4C1, OATP5A1 and OATP6A1, we used XbaI for linearization. OATP1C1 was linearized with Acc65I, and OATP2A1 was linearized with DraI. All restriction enzymes were obtained from Fermentas. After linearization, proteinase K and 0.5% SDS treatment, plasmid DNA was purified by phenol/chloroform extraction and ethanol precipitation. OATP1A2 and OATP2B1 sequences were amplified from the plasmids using 0.5 mM of dNTPs, 12.5 pmol of each primer, 0.75 µl DMSO, 0.5 U Hot Start Phusion® DNA polymerase (Finnzymes) and 1x GC buffer (Finnzymes) in a final volume of 25 µl. Standard vector primers (M13) were used for amplification: forward: 5'-TGT AAA ACG ACG GCC AGT-3' and reverse: 5'- CAG GAA ACA GCT ATG ACC-3'. Thermal cycling conditions were as follows: 98 ℃ f or 30 s, 25 cycles of 98 ℃ for 15 s, 55 ℃ for 20 s and 72 ℃ for 1 min on a Bio-Rad MyC ycler™. The obtained OATP1A2 and OATP2B1 PCR products were gel-purified and used as templates for *in vitro* transcription. 5'-capped cRNAs were transcribed *in vitro* using 1 µg of template DNA and either T7 or SP6 mMESSAGE mMACHINE® kit (Ambion, Austin, TX) according to the manufacturer's instructions. Subsequently, the cRNAs were polyA-tailed using the polyA tailing kit (Ambion) according to the protocol. The polyA cRNA was then purified using the MEGAClear™ kit (Ambion). The concentration, purity and integrity of cRNA samples were determined on a Nanodrop ND-1000 (Kisker-Biotech) and by denaturing gel electrophoresis.

2.9. Paclitaxel transport studies in Xenopus laevis oocytes

Preparation of stage V-VI oocytes from *X. laevis* was performed as previously described [34]. Briefly, *X. laevis* frogs (NASCO, USA) were anaesthetized by exposing them for 15 min to a 0.2% solution of MS-222 (methane sulfonate salt of 3-aminobenzoic acid ethyl ester; Sandoz Company) before surgical removal of parts of the ovaries. Follicle membranes from isolated oocytes were enzymatically digested with 2 mg/ml collagenase (Type 1A, Sigma). One day after isolation, the oocytes were injected with either 10 - 50 nl of water to determine non-specific uptake of paclitaxel or water with approximately 200 ng/µl cRNA of each OATP. Injected oocytes were incubated in ND96 buffer (90 mM NaCl, 1 mM KCl, 1 mM $MgCl_2$, 1 mM $CaCl_2$, and 5 mM HEPES, pH adjusted to 7.4, supplemented with 100 U/ml penicillin and 100 µg/ml streptomycin) at 18 ℃ for 48 hours before performing transport expe riments with buffer exchange every day. Uptake studies were carried out in single oocytes using at least 12 oocytes per data point. Oocytes were washed three times with 3 ml substrate-free uptake buffer (100 mM NaCl, 2 mM KCl, 1 mM $MgCl_2$, 1 mM $CaCl_2$, 10 mM HEPES, pH adjusted to 7.4 with TRIS) and incubated with 400 µl uptake buffer containing 20 nM [^{3}H]paclitaxel and 1% ethanol at room temperature for the appropriate time points. To avoid unspecific binding of [^{3}H]paclitaxel to the surfaces of laboratory plasticware, all solutions containing [^{3}H]paclitaxel were manipulated using glassware. For kinetic analysis, the uptake of radiolabeled paclitaxel was measured over a range of concentrations, from 20 to 1180 nM, using 60-min incubations within the linear component of uptake. Uptake was corrected for non-specific influx using water-injected oocytes from the same batch in each experiment. Uptake was stopped by the addition of 3 ml ice-cold uptake buffer, and oocytes were washed three times with buffer before being placed in scintillation vials for dissolution with 10% SDS overnight. Radioactivity was measured in a liquid scintillation counter (LS-6500; Beckman, California, USA).

2.10. Western blot analysis of OATP1B1 and 1B3 in X. laevis *oocytes*

Oocyte protein expression and membrane localization of human OATP1B1 and OATP1B3 were confirmed by western blot using membrane and cytosolic protein fractions from OATP1B1- and OATP1B3-injected oocytes [35]. A total of 10 µg of protein was separated on 10% separating gels, blotted on PVDF membranes and probed using an antibody against OATP1B1/1B3 (#BM5541, Acris) diluted 1:250 in TBS-T (20 mM Tris, 145 mM NaCl, 0.05% Tween 20, pH 7.6) containing 5% milk powder [36]. On control blots, an antibody to α-tubulin (Sigma, T-5168) was diluted 1:8000 in TBS-T containing 5% milk powder. The HRP-conjugated secondary antibody (#315-036-003, Jackson ImmunoResearch, Suffolk, UK) was used at a dilution of 1:10000 in TBS-T.

2.11. Transport experiments in OVCAR-3 *and* SK-OV-3 *cells*

Cells that were 80-90% confluent were washed three times and incubated for 15 min (37 °C) in 12-well plates with 1 ml Krebs-Henseleit buffer (KHB, 118 mM NaCl, 23.8 mM $NaHCO_3$, 4.8 mM KCl, 1.0 mM KH_2PO_4, 1.2 mM $MgSO_4$, 12.5 mM HEPES, 5.0 mM glucose, and 1.5 mM $CaCl_2$, pH 7.4) (Hirano et al. 2004). Subsequently, cells were treated with 1 ml/well KHB containing 18.5 nM [^{3}H] paclitaxel. Unlabeled paclitaxel was added to a final concentration of 5 µM. Uptake was measured after 1, 2, 4, 6 and 10 min or, alternatively, at graded concentrations (0.5, 1.0, 2.5, 5.0 and 10.0 µM paclitaxel) after 1 min of incubation, which had been determined to be within the linear range of uptake. Control studies were performed at 4 °C to determine temperature-insensitive paclitaxel accumulation. Paclitaxel transport was stopped by adding ice-cold KHB followed by three washes. The amount of paclitaxel in the cells was determined by first adding 300 µl 0.2 N NaOH to each well. After 12 h at 4 °C, 150 µl 0.4 N HCl and 4 ml Emulsifier-Safe™ scintillation cocktail (PerkinElmer) were added, and [^{3}H]paclitaxel

uptake was measured in an LS6500 scintillation counter (Beckman Coulter, Fullerton, CA). Protein determination was performed using a BCA™ Protein Assay (Pierce, Rockford, IL), with bovine serum albumin as the standard.

2.12. Data analysis

For kinetic analysis, data were fitted to the Michaelis-Menten (hyperbolic) model. Kinetic parameters were estimated using Prism 5 software (GraphPad) for Michaelis-Menten kinetics:

$$V=V_{max}\cdot S/(K_m+S),$$

where V is the rate of reaction, V_{max} is the maximum velocity, K_m is the Michaelis constant, and S is the substrate concentration. Unless otherwise indicated, values are expressed as the mean ± SD of at least 12 individual oocytes per data point. Statistical differences from control values were evaluated using a Student's t-test, and the level of statistical significance was set at $P < 0.05$.

3. Results

3.1. Expression of OATPs in human ovarian cancer specimens

To assess the role of OATP transporters for paclitaxel uptake, we investigated the mRNA expression of all 11 human OATPs in a series of ovarian cancer tissue samples using TaqMan® real-time RT-PCR. Total RNA from normal ovary served as control. As shown in Table 3, mRNA of all 11 OATPs was observed in specimens of ten ovarian cancer patients at quite different levels (from 0.02-fold to 103-fold compared to the endogenous control gene *HPRT1*), whereas in normal ovaries, mRNA expression was confined to five OATP family members (OATP2A1, OATP2B1, OATP3A1, OATP4A1 and OATP5A1). In normal ovary tissue, OATP1B1 and OATP1B3 mRNA expression

was below the detection limit, whereas OATP1B3 was clearly detected in 5/10 ovarian cancer specimens. Interestingly, three of the five OATP1B3-expressing samples also expressed OATP1B1. These data were confirmed by immunohistochemistry, demonstrating that protein levels of OATP1B1 and 1B3 correlate with mRNA expression in cancerous tissue (a representative tumor sample is shown in Fig. 1A). In line with real-time RT-PCR, no staining for these proteins was observed in noncancerous tissue (Fig. 1B).

3.2. OATP mRNA expression in ovarian cancer cells

We further investigated the mRNA expression profile of all human OATPs in the human ovarian carcinoma cell lines OVCAR-3 and SK-OV-3. Interestingly, expression of the liver-specific OATP1B3 mRNA was up to 204-fold higher in SK-OV-3 cells compared to OVCAR-3 cells (Table 4). Even more pronounced was the difference in OATP1B1 expression, as this transporter was only found in SK-OV-3 cells. A different expression pattern was also observed for OATP2B1, which was 71-fold higher in SK-OV-3 cells, and for OATP5A1, which was 85-fold higher in the OVCAR-3 cell line. mRNA expression of OATP1A2, OATP2A1, OATP3A1, OATP4A1 and OATP4C1 was detected in OVCAR-3 and SK-OV-3, although the observed distribution was more balanced. Expression levels of OAT2 (previously identified as a potential paclitaxel transporter) [26], OATP1C1 and OATP6A1 were below the detection limit in both cell lines.

3.3. Expression of paclitaxel efflux transporters in ovarian cancer cell lines

Despite differing expression of OATP1B1 and OATP1B3, OVCAR-3 and SK-OV-3 cells displayed similar paclitaxel cytotoxicity. As overexpression of OATP increased the cytotoxicity of paclitaxel, the comparable sensitivity of naive OVCAR-3 cells to paclitaxel could be influenced by the different expression levels of efflux pumps. Therefore, we

further investigated the expression of four major paclitaxel efflux transporters in these two cell lines. We indeed observed up to 18-fold higher mRNA expression levels for MRP2 and MRP3 in SK-OV-3 cells (Table 5), suggesting a higher efflux of paclitaxel out of the cytoplasm into the cellular supernatant. MDR1 and MRP7 were similar in distribution between the two cell lines.

3.4. Paclitaxel transport studies in X. laevis oocytes

To investigate whether OATPs other than OATP1B3 contribute to paclitaxel uptake into OVCAR-3 and SK-OV-3 cells, uptake studies were performed for all 11 known human OATPs in *X. laevis* oocytes injected with cRNA coding for each of the OATP family members. Uptake of radiolabeled paclitaxel (20 nM for 60 min) in OATP1B1- and OATP1B3-expressing oocytes was significantly higher compared to the water-injected oocytes (5.3- and 3.9-fold, respectively; $P < 0.0001$). No other OATP favored paclitaxel uptake (Fig. 2). The time course of [^{3}H]paclitaxel uptake by OATP1B1- and OATP1B3-expressing oocytes was linear for up to 60 min (Figs. 3A and B). The kinetic constants for this uptake revealed saturable transport in OATP1B1-expressing oocytes, with a V_{max} of 12.3 ± 0.4 fmol/oocyte/min and a K_m value of 0.6 ± 0.04 µM. OATP1B3-injected oocytes showed a 2.4-fold higher V_{max} for paclitaxel (30 ± 1.6 fmol/oocyte/min) and a 2.7-fold higher K_M value of 1.6 ± 0.13 µM compared to OATP1B1-injected oocytes (Figs. 3C and D). OATP1B1 and OATP1B3 protein expression in *X. laevis* oocyte plasma membranes was also confirmed by western blot analysis (Figs. 3E and F). Involvement of both transporters for paclitaxel uptake was also confirmed in inhibition experiments by using the OATP1B1 and 1B3 substrate [^{3}H]estrone-3-sulfate. Paclitaxel (2 µM) reduced intracellular accumulation of 20 nM [^{3}H]estrone-3-sulfate in OATP1B1- and OATP1B3-expressing *X. laevis* oocytes to 44.1 ± 5.0 % and 63.0 ± 7.3 %, respectively, further confirming uptake by these transporters.

3.5. Transport of paclitaxel in ovarian cancer cell lines

Based on the different expression levels of OATPs in OVCAR-3 and SK-OV-3 cells, we also expected altered intracellular paclitaxel levels. In both cell lines, uptake of paclitaxel was linear with time, up to 90 sec, with respect to 5 µM paclitaxel concentrations (data not shown). For kinetic analysis, an incubation time of 1 min was therefore chosen, showing typical Michaelis-Menten kinetics for the uptake of paclitaxel into the OVCAR-3 cells, with a V_{max} of 517.5 ± 86.2 pmol/mg protein/min and a K_m value of 17.2 ± 4.1 µM (Fig. 4A). Transport of paclitaxel into the SK-OV-3 cell line was far more pronounced, showing an uptake rate of 1660 ± 126 pmol/mg protein/min at a concentration of 10 µM. Because of the limited solubility of this drug in serum-containing cell culture medium, saturation kinetics could not be observed (Fig. 4B).

3.6. Paclitaxel cytotoxicity in OATP1B1- and OATP1B3-transfected SK-OV-3 cells

To investigate whether increased expression of either OATP1B1 or OATP1B3 could have an impact on paclitaxel cytotoxicity we tested the efficacy of paclitaxel in OATP1B1- and OATP1B3-transfected SK-OV-3 cells. As shown in Fig. 5, the IC_{50} was decreased to 2.8 ± 1.38 nM for paclitaxel in OATP1B1 cells and to 3.4 ± 1.27 nM in OATP1B3 cells (compared to 4.9 ± 1.35 nM in cells transfected with the empty vector).

4. Discussion and conclusion

In the present study, we elucidated the transcriptional expression for human OATPs in malignant and control ovarian tissue samples and in estrogen-responsive OVCAR-3 and estrogen-independent SK-OV-3 ovarian cancer cell lines,

By investigation of all 11 known OATPs by TaqMan® real-time RT-PCR, we found that OATP1B1, OATP1B3 and OATP2B1 were highly expressed in SK-OV-3 cells, whereas OATP1A2, OATP4C1 and OATP5A1 were primarily present in OVCAR-3 cells.

The two transporters OATP1C1 and OATP6A1 were not detectable in either cell line. It should be noted that expression of OAT2, which was previously shown to mediate the uptake of paclitaxel in *X. laevis* oocytes, was below the detection limit in both cell lines. Our data are consistent with the previous work of Okabe and coworkers, who showed similar differences of OATP expression in OVCAR-3 and SK-OV-3 cells [24]. However, contrary to their study, we were unable to confirm expression of OATP6A1 in the OVCAR-3 cell line.

To date, the only OATP that has been characterized as a high-affinity paclitaxel transporter [25] is OATP1B3. Uptake of paclitaxel was significantly reduced in the OATP1B3-expressing cell line HepG2 but not in OATP1B3-deficient PR-HepG2 cells by the OATP1B3 substrate and inhibitor bromosulfophtalein [37]. By systematically investigating the transport properties of paclitaxel for all 11 OATPs using the *X. laevis* oocytes expression system, we were able to identify OATP1B1 as an additional uptake protein for paclitaxel. Indirect involvement of OATP1B1 in taxane transport was reported by Gui and coworkers who showed inhibition of the OATP1B1 substrate estradiol-17β-glucuronide by paclitaxel in stable transfected CHO cells [38]. An involvement of OATP1B1 in hepatic clearance of paclitaxel may explain the finding of a pharmacogenetic investigation of variants of the *SLCO1B3* gene; Smith and coworkers found that differences in paclitaxel pharmacokinetics did not correlate with different OATP1B3 variants [39]. Nevertheless, one variant has recently been shown to influence the pharmacokinetics of mycophenolate [40].

Several ABC transporters have been shown to successfully expel paclitaxel from the cells. Importantly, it has been demonstrated that MDR1 and MRP2, as well as MRP3 and MRP7, mediate paclitaxel transport [7-10]. However, exposing SK-OV-3 cells transiently overexpressing OATP1B1 and OATP1B3 to paclitaxel decreased their IC_{50}, indicating that the sensitivity of the ovarian cancer cells to paclitaxel can be

modulated by OATP1B1/1B3 expression levels. Using TaqMan® real-time RT-PCR, we identified higher expression levels of MRP2 and MRP3 in SK-OV-3 cells, whereas differences of MDR1 and MRP7 mRNA expression were moderate. MRP2 and MRP3 may therefore facilitate increased efflux of paclitaxel in SK-OV-3 cells.

Our data suggest that OATP1B1 might be an even more important determinant of paclitaxel uptake in ovarian cancer cells than OATP1B3, based on its lower K_m value in *X. laevis* oocytes (0.6 µm vs. 1.6 µM). This K_m is in the range of the mean plasma concentration in patients (0.85 ± 0.21 µM) after 24 h of infusion [41]. Our conclusion that paclitaxel could be a better substrate for OATP1B1than OATP1B3 is supported by very recent experiments of Gui and coworkers as they found that paclitaxel (2.5 µM) inhibited the uptake of the OATP1B1/1B3 substrate fluorescein-methotrexate by 93% in OATB1B1- but only by 53% in OATP1B3-expressing CHO cells [42]. Differences in estrogen-responsive and estrogen-independent ovarian cancer cell lines also suggest that alterations in mRNA expression levels may also be observed in tumor tissue samples from patients. It is known that the activity and the expression of transport proteins may vary greatly between individuals, as a function of genetic, environmental, and physiological factors. Indeed, we also demonstrated great differences in the expression of all 11 OATPs in 10 ovarian cancer specimens and one control tissue sample (Table 3). Among these polypeptides, expression of OATP1A2, OATP1B1, OATP1B3, OATP1C1, and OATP6A1 was found exclusively in the tumor samples but not in the control one.

OATP1B1- and OATP1B3-mediated paclitaxel transport may be of clinical importance, as our data show for the first time that both transporters are also expressed in ovarian cancer specimens but not in control tissue. This expression is remarkable, since OATP1B1 and OATP1B3 are proposed to be expressed under normal conditions in liver only [14]. As the expression of both OATPs are positively regulated by the transcription

factor HNF1α [43], any upregulation of HNF1α may subsequently increase OATP1B1 and 1B3 levels. Indeed, Tomassetti and coworker demonstrated that vHNF1 (the variant isoform of the hepatocyte nuclear factor 1) is highly expressed in cancer tissue but not in normal ovarian epithelium [44].

OATP1B1 and OATP1B3 share a wide, overlapping substrate spectrum that includes HMG-CoA reductase inhibitors such as fluvastatin and pitavastatin, the antibiotic rifampicin and the endothelin receptor antagonist BQ123 [45]. The hepatic uptake rate of both transporters might be reduced by drug competition, resulting in increased blood levels. Therefore, inter-individual expression levels of OATP1B1 and OATP1B3 in the basolateral membrane of hepatocytes might be responsible for differences in the occurrence of toxic side effects such as neutropenia, neuropathy and cardiac effects during paclitaxel therapy. Such drug-drug interactions have been reported for the OATP1B1 and OATP1B3 substrates pravastatine and bosentan [46,47] when concomitantly administered with clarithromycin and cyclosporine or rifampicin, respectively.

In conclusion, we found that OATP1B1 and OATP1B3 are high affinity and active paclitaxel transporters in transfected *X. laevis* oocytes; this role may also apply for the uptake of this compound into human liver and ovarian cancer cells.

Conflict of interest statement

There is no conflict of interest

Acknowledgements

This study was supported by FP-6 STREP Project (OVCAD 2005-018698), the Jubiläumsfonds der Österreichischen Nationalbank (12600 to W.J.). K.W. thanks the Austrian Academy of Science for a DOC-fFORTE fellowship.

References

[1] DiSaia, P.J., Creasman, W.T., 2002, Epithelial Ovarian Cancer, in: P.J. DiSaia, W.T.Creasman (Eds.), Clinical gynecologic oncology. 6th ed. St. Louis: Mosby-Year Book, 289-350.

[2] Permuth-Wey J, Sellers TA. Epidemiology of ovarian cancer. Methods Mol Biol. 2009;472:413-37.

[3] Rowinsky EK, Donehower RC. Paclitaxel (taxol). N Engl J Med. 1995 ;332:1004-14.

[4] Agarwal R, Kaye SB. Ovarian cancer: strategies for overcoming resistance tochemotherapy. Nat Rev Cancer. 2003;3:502-16.

[5] Markman M. Antineoplastic agents in the management of ovarian cancer: current status and emerging therapeutic strategies. Trends Pharmacol Sci. 2008;29:515-9.

[6] Baekelandt MM, Holm R, Nesland JM, Tropé CG, Kristensen GB. P-glycoproteinexpression is a marker for chemotherapy resistance and prognosis in advancedovarian cancer. Anticancer Res. 2000;20:1061-7.

[7] Kamazawa S, Kigawa J, Kanamori Y, Itamochi H, Sato S, Iba T, Terakawa N. Multidrug resistance gene-1 is a useful predictor of Paclitaxel-based chemotherapy for patients with ovarian cancer. Gynecol Oncol. 2002;86:171-6.

[8] Huisman MT, Chhatta AA, van Tellingen O, Beijnen JH, Schinkel AH. MRP2 (ABCC2) transports taxanes and confers paclitaxel resistance and both processes are stimulated by probenecid. Int J Cancer. 2005;116:824-9.

[9] O'Brien C, Cavet G, Pandita A, Hu X, Haydu L, Mohan S, Toy K, Rivers CS, Modrusan Z, Amler LC, Lackner MR. Functional genomics identifies ABCC3 as a mediator of taxane resistance in HER2-amplified breast cancer. Cancer Res. 2008;68:5380-9.

[10] Oguri T, Ozasa H, Uemura T, Bessho Y, Miyazaki M, Maeno K, Maeda H, Sato S, Ueda R. MRP7/ABCC10 expression is a predictive biomarker for the resistance to paclitaxel in non-small cell lung cancer. Mol Cancer Ther. 2008;7:1150-5.

[11] Dobson PD, Kell DB. Carrier-mediated cellular uptake of pharmaceutical drugs: an exception or the rule? Nat Rev Drug Discov. 2008;7:205-20.

[12] Hagenbuch B, Gui C. Xenobiotic transporters of the human organic anion transporting polypeptides (OATP) family. Xenobiotica. 2008;38:778-801.

[13] Kim RB. Organic anion-transporting polypeptide (OATP) transporter family and drug disposition. Eur J Clin Invest. 2003;33 Suppl 2:1-5.

[14] Hagenbuch B, Meier PJ. Organic anion transporting polypeptides of the OATP/SLC21 family: phylogenetic classification as OATP/ SLCO superfamily, new nomenclature and molecular/functional properties. Pflugers Arch. 2004;447:653-65.

[15] Tamai I, Nezu J, Uchino H, Sai Y, Oku A, Shimane M, Tsuji A. Molecular identification and characterization of novel members of the human organic anion transporter (OATP) family. Biochem Biophys Res Commun. 2000;273:251-60.

[16] Muto M, Onogawa T, Suzuki T, Ishida T, Rikiyama T, Katayose Y, Ohuchi N, Sasano H, Abe T, Unno M. Human liver-specific organic anion transporter-2 is a potent prognostic factor for human breast carcinoma. Cancer Sci. 2007;98:1570-6.

[17] Wlcek K, Svoboda M, Thalhammer T, Sellner F, Krupitza G, Jaeger W. Altered expression of organic anion transporter polypeptide (OATP) genes in human breast carcinoma. Cancer Biol Ther. 2008;7:1450-5.

[18] Mikkaichi T, Suzuki T, Tanemoto M, Ito S, Abe T. The organic anion transporter (OATP) family. Drug Metab Pharmacokinet. 2004;19:171-9.

[19] Abe T, Unno M, Onogawa T, Tokui T, Kondo TN, Nakagomi R, Adachi H, Fujiwara K, Okabe M, Suzuki T, Nunoki K, Sato E, Kakyo M, Nishio T, Sugita J, Asano N, Tanemoto M, Seki M, Date F, Ono K, Kondo Y, Shiiba K, Suzuki M, Ohtani H, Shimosegawa T, Iinuma K, Nagura H, Ito S, Matsuno S. LST-2, a human liver-specific organic anion transporter, determines methotrexate sensitivity in gastrointestinal cancers. Gastroenterology. 2001;120:1689-99.

[20] Okabe M, Unno M, Harigae H, Kaku M, Okitsu Y, Sasaki T, Mizoi T, Shiiba K, Takanaga H, Terasaki T, Matsuno S, Sasaki I, Ito S, Abe T. Characterization of the organic cation transporter SLC22A16: a doxorubicin importer. Biochem Biophys Res Commun. 2005;333:754-62.

[21] Ciarimboli G, Ludwig T, Lang D, Pavenstädt H, Koepsell H, Piechota HJ, Haier J, Jaehde U, Zisowsky J, Schlatter E. Cisplatin nephrotoxicity is critically mediated via the human organic cation transporter 2. Am J Pathol. 2005;167:1477-84.

[22] Yonezawa A, Masuda S, Yokoo S, Katsura T, Inui K. Cisplatin and oxaliplatin, but not carboplatin and nedaplatin, are substrates for human organic cation transporters (SLC22A1-3 and multidrug and toxin extrusion family). J PharmacolExp Ther. 2006;319:879-86.

[23] Zhang S, Lovejoy KS, Shima JE, Lagpacan LL, Shu Y, Lapuk A, Chen Y, Komori T,Gray JW, Chen X, Lippard SJ, Giacomini KM. Organic cation transporters are determinants of oxaliplatin cytotoxicity. Cancer Res. 2006;66:8847-57.

[24] Okabe M, Szakács G, Reimers MA, Suzuki T, Hall MD, Abe T, Weinstein JN, Gottesman MM. Profiling SLCO and SLC22 genes in the NCI-60 cancer cell lines to identify drug uptake transporters. Mol Cancer Ther. 2008;7:3081-91.

[25] Smith NF, Acharya MR, Desai N, Figg WD, Sparreboom A. Identification of OATP1B3 as a high-affinity hepatocellular transporter of paclitaxel. Cancer Biol Ther. 2005;4:815-8.

[26] Kobayashi Y, Ohshiro N, Sakai R, Ohbayashi M, Kohyama N, Yamamoto T. Transport mechanism and substrate specificity of human organic anion transporter 2 (hOat2 [SLC22A7]). J Pharm Pharmacol. 2005;57:573-8.

[27] Sekine T, Cha SH, Tsuda M, Apiwattanakul N, Nakajima N, Kanai Y, Endou H. Identification of multispecific organic anion transporter 2 expressed predominantly in the liver. FEBS Lett. 1998;429:179-82.

[28] van de Steeg E, van Esch A, Wagenaar E, van der Kruijssen CM, van Tellingen O,Kenworthy KE, Schinkel AH. High impact of Oatp1a/1b transporters on in vivodisposition of the hydrophobic anticancer drug paclitaxel. Clin Cancer Res. 2011;17:294-301.

[29] Kang SK, Choi KC, Tai CJ, Auersperg N, Leung PC. Estradiol regulates gonadotropin-releasing hormone (GnRH) and its receptor gene expression and antagonizes the growth inhibitory effects of GnRH in human ovarian surface epithelial and ovarian cancer cells. Endocrinology. 2001;142:580-8.

[30] Keith Bechtel M, Bonavida B. Inhibitory effects of 17beta-estradiol and progesterone on ovarian carcinoma cell proliferation: a potential role for nducible nitric oxide synthase. Gynecol Oncol. 2001;82:127-38.

[31] Shepherd JH. Revised FIGO staging for gynaecological cancer. Br J Obstet Gynaecol. 1989;96:889-92.

[32] Livak KJ, Schmittgen TD. Analysis of relative gene expression data using real-time quantitative PCR and the 2(-Delta Delta C(T)) Method. Methods. 2001;25:402-8.

[33] Kullak-Ublick GA, Ismair MG, Stieger B, Landmann L, Huber R, Pizzagalli F, Fattinger K, Meier PJ, Hagenbuch B. Organic anion-transporting polypeptide B (OATP-B) and its functional comparison with three other OATPs of human liver. Gastroenterology. 2001;120:525-33.

[34] Khom S, Baburin I, Timin EN, Hohaus A, Sieghart W, Hering S. Pharmacological properties of GABAA receptors containing gamma1 subunits. Mol Pharmacol. 2006;69:640-9.

[35] Bianchi L, Driscoll M. Heterologous expression of C. elegans ion channels in Xenopus oocytes. WormBook. 2006 Aug 1:1-16.

[36] Cui Y, König J, Nies AT, Pfannschmidt M, Hergt M, Franke WW, Alt W, Moll R, Keppler D. Detection of the human organic anion transporters SLC21A6 (OATP2) and SLC21A8 (OATP8) in liver and hepatocellular carcinoma. Lab Invest. 2003;83:527-38.

[37] Takano M, Otani Y, Tanda M, Kawami M, Nagai J, Yumoto R. Paclitaxel-resistance conferred by altered expression of efflux and influx transporters for paclitaxel in the human hepatoma cell line, HepG2. Drug Metab Pharmacokinet. 2009;24:418-27.

[38] Gui C, Miao Y, Thompson L, Wahlgren B, Mock M, Stieger B, Hagenbuch B. Effect of pregnane X receptor ligands on transport mediated by human OATP1B1 and OATP1B3. Eur J Pharmacol. 2008;584:57-65.

[39] Smith NF, Marsh S, Scott-Horton TJ, Hamada A, Mielke S, Mross K, Figg WD, Verweij J, McLeod HL, Sparreboom A. Variants in the SLCO1B3 gene: interethnic distribution and association with paclitaxel pharmacokinetics. Clin Pharmacol Ther. 2007;81:76-82.

[40] Picard N, Yee SW, Woillard JB, Lebranchu Y, Le Meur Y, Giacomini KM, Marquet P. The role of organic anion-transporting polypeptides and their common genetic variants in mycophenolic acid pharmacokinetics. Clin Pharmacol Ther. 2010;87:100-8.

[41] Sonnichsen DS, Relling MV. Clinical pharmacokinetics of paclitaxel. Clin Pharmacokinet. 1994;27:256-69.

[42] Gui C, Obaidat A, Chaguturu R, Hagenbuch B. Development of a cell-based high-throughput assay to screen for inhibitors of organic anion transporting polypeptides 1B1 and 1B3. Curr Chem Genomics. 2010;4:1-8.

[43] Jung D, Hagenbuch B, Gresh L, Pontoglio M, Meier PJ, Kullak-Ublick GA. Characterization of the human OATP-C (SLC21A6) gene promoter and regulation of liver-specific OATP genes by hepatocyte nuclear factor 1 alpha. J Biol Chem. 2001;276:37206-14.

[44] Tomassetti A, De Santis G, Castellano G, Miotti S, Mazzi M, Tomasoni D, Van Roy F, Carcangiu ML, Canevari S. Variant HNF1 modulates epithelial plasticity of normal and transformed ovary cells. Neoplasia. 2008;10:1481-92, 3p following 1492.

[45] König J, Seithel A, Gradhand U, Fromm MF. Pharmacogenomics of human OATP transporters. Naunyn Schmiedebergs Arch Pharmacol. 2006;372:432-43.

[46] Seithel A, Eberl S, Singer K, Auge D, Heinkele G, Wolf NB, Dörje F, Fromm MF, König J. The influence of macrolide antibiotics on the uptake of organic anions and drugs mediated by OATP1B1 and OATP1B3. Drug Metab Dispos. 2007;35:779-86.

[47] Treiber A, Schneiter R, Häusler S, Stieger B. Bosentan is a substrate of human OATP1B1 and OATP1B3: inhibition of hepatic uptake as the common mechanism of its interactions with cyclosporin A, rifampicin, and sildenafil. Drug Metab Dispos. 2007;35:1400-7.

Legends to the Figures

Fig. 1: Representative images of immunohistochemistry stainings using an OATP1B1/OATP1B3 specific antibody in ovarian tissue. In the ovarian carcinoma image of patient no. 2 (A) clear immunoreactivity with the antibody is seen, whereas no staining is observed in non-cancerous ovarian tissue (B).

Fig. 2: Paclitaxel uptake in *X. laevis* oocytes. The uptake of [^{3}H]paclitaxel was measured in *X. laevis* oocytes injected with human OATP cRNA after a 60-min incubation with 20 nM [^{3}H]paclitaxel. Data are given as the percent of controls ± SD of at least 12 oocytes per data point. OATPs showing significantly higher (***$P < 0.001$) uptake rates compared to water-injected oocytes (control) are marked with asterisks.

Fig. 3: Time- and concentration-dependent uptake of paclitaxel by OATP1B1- and OATP1B3-expressing *X. laevis* oocytes. The time-dependent uptake of 20 nM [^{3}H]paclitaxel was measured for OATP1B1 (A) and OATP1B3 (B) cRNA-injected oocytes. Water-injected *X. laevis* oocytes were included as a negative control.

Concentration-dependent paclitaxel uptake for OATP1B1- (C) and OATP1B3-expressing oocytes (D) was evaluated after an incubation time of 60 min with various paclitaxel concentrations ranging from 20 to 1180 nM. Data represent the mean ± SD of triplicate determinations. Protein expression of OATP1B1 (E) and 1B3 (F) in *X. laevis* oocytes was confirmed by western blot analysis of cRNA-injected (+) and water-injected (-) oocytes.

Fig. 4: Time- and concentration-dependent uptake of paclitaxel in the ovarian cancer cell lines OVCAR-3 and SK-OV-3. The time-dependent uptake of 5 µM paclitaxel was measured in OVCAR-3 (A) and SK-OV-3 (B) cells at 1, 2, 4, 6 and 10 min. Concentration-dependent paclitaxel uptake in OVCAR-3 (C) and SK-OV-3 (D) cells was evaluated after an incubation time of 1 min at 4℃ and 37℃ with paclitaxel concentrations ranging from 0.5 to 10 µM. Kinetic constants were calculated by non-linear least-square analysis. Data represent the mean ± SD of triplicate determinations.

Fig. 5: Cytotoxic effect of paclitaxel. An ATP-based detection assay was used to assess paclitaxel cytotoxicity in with OATP1B1, OATP1B3, and empty vector transiently transfected SK-OV-3 cells. Eight measurements were performed for each dilution point (mean ± SD).

Table 1

Tumor characteristics of patients

Patient no.	Age (y) at first diagnosis	Number of relapses	FIGOa	Tb	Nb	Mb	Grade
1	62	1	IV	3b	N1	M1	II
2	40	3	IIIC	3c	NX	MX	II
3	47	6	IIC	2c	N0	MO	III
4	39	2	IIIC	1c	N1	MO	II
5	55	3	IIIC	3c	NX	MX	III
6	42	2	IIIC	3c	NX	MX	IV
7	52	2	IIA	2a	NX	M0	II
8	64	2	IC	1c	NX	MO	III
9	57	2	IIIC	3c	NX	MX	II
10	44	2	IIIC	3c	N1	MO	III

[a]According to the International Federation of Gynecologists & Obstetricians (FIGO); [b]According to the International Union Against Cancer (UICC) Tumor, Node Metastasis (TNM) classification.

Table 2

Overview of the applied gene expression assays (ABI) used for real-time RT-PCR analysis

Protein name	Assay ID[a]	Context sequence (5'→3')	Accession number
OATP1A2	hs00245360_m1	ACCACCTTCAGATACATCTACCTCG	NM_134431.2 NM_021094.2
OATP1B1	hs00272374_m1	ATTCCACATCATTTTCAAGGGTCTA	NM_006446.3
OATP1B3	hs00251986_m1	CTAACTTTTTGTTGGGAATCATAAC	NM_019844.2
OATP1C1	hs00213714_m1	CTCCTACCAAGGAACCAAACCTGTC	NM_017435.3
OATP2A1	hs00194554_m1	GCGCTTGCTGGCCTGGCTGCCATCT	NM_005630.1
OATP2B1	hs00200670_m1	CTGCCAGGAAGGGCAAGGACTCTCC	NM_007256.2
OATP3A1	hs00203184_m1	CTCCTCGCTCTATATAGGAATCCTG	NM_013272.2
OATP4A1	hs00249583_m1	CAGAGACCTGCCTCTCTCCATCTGG	NM_016354.3
OATP4C1	hs00698884_m1	TGGGAGAAAGCACTGATGTCACTGA	NM_180991.4
OATP5A1	hs00229597_m1	TCATTGGAAACTGGTGGAGTGGATT	NM_030958.1
OATP6A1	hs00542846_m1	CTACACTTGCAGGACTTGTTTTAAT	NM_173488.3
OAT2	hs00198527_m1	AGCCTCTGGTGGGTGCCTGAGTCTG	NM_153320.2 NM_006672.3
MDR1	hs00184500_m1	AGACATGACCAGGTATGCCTATTAT	NM_000927.3
MRP2	hs00166123_m1	CACCTCCAACAGGTGGCTTGCAATT	NM_000392.3
MRP3	hs00358656_m1	CAGCTGCTCAGCATCCTGATCAGGT	NM_001144070.1 NM_003786.3
MRP7	hs00375716_m1	CCCAGCTCAGATCCCAGTTGGCTAT	NM_033450.2

[a]Applied Biosystems

Table 3

Expression levels of OATP mRNA in normal (N) and ovarian cancer specimens[a]

Gene symbol	N	1	2	3	4	5	6	7	8	9	10
OATP1A2	ND	**1,31 ± 0,11**	0,08 ± 0,00	ND	0,02 ± 0,01	0,48 ± 0,02	0,13 ± 0,10	0,04 ± 0,00	0,04 ± 0,00	0,2 ± 0,0	ND
OATP1B1	ND	ND	**2,33 ± 0,33**	ND	1,19 ± 0,06	ND	ND	ND	ND	ND	0,4 ± 0,0
OATP1B3	ND	ND	1,27 ± 0,08	ND	**2,18 ± 0,30**	ND	0,06 ± 0,01	ND	0,04 ± 0,00	ND	1,1 ± 0,0
OATP1C1	ND	ND	0,04 ± 0,00	ND	ND	ND	ND	ND	**0,10 ± 0,00**	ND	ND
OATP2A1	**4,35 ± 0,15**	0,96 ± 0,30	3,03 ± 0,29	1,02 ± 0,14	1,03 ± 0,04	1,33 ± 0,25	3,05 ± 0,39	0,37 ± 0,01	2,02 ± 0,14	0,31 ± 0,01	0,42 ± 0,05
OATP2B1	**103 ± 2,02**	1,13 ± 0,09	9,36 ± 1,14	4,90 ± 0,39	3,91 ± 0,27	7,23 ± 0,36	32,4 ± 6,86	3,32 ± 0,24	5,50 ± 0,57	4,19 ± 0,35	3,33 ± 0,29
OATP3A1	1,88 ± 0,04	**2,76 ± 0,12**	1,23 ± 0,14	1,45 ± 0,16	1,25 ± 0,08	1,48 ± 0,07	1,34 ± 0,13	0,19 ± 0,01	2,03 ± 0,16	1,56 ± 0,13	1,54 ± 0,13
OATP4A1	0,36 ± 0,01	0,22 ± 0,01	0,50 ± 0,03	0,31 ± 0,01	**1,22 ± 0,05**	0,07 ± 0,00	1,00 ± 0,28	0,02 ± 0,00	0,12 ± 0,01	0,06 ± 0,01	0,08 ± 0,00
OATP4C1	0,02 ± 0,00	0,05 ± 0,02	0,05 ± 0,01	0,03 ± 0,01	0,04 ± 0,00	0,02 ± 0,01	**0,67 ± 0,09**	0,03 ± 0,00	0,15 ± 0,00	0,04 ± 0,00	ND
OATP5A1	0,41 ± 0,06	**1,34 ± 0,41**	0,62 ± 0,08	0,12 ± 0,02	0,25 ± 0,04	0,63 ± 0,12	0,12 ± 0,06	0,09 ± 0,00	0,29 ± 0,03	0,13 ± 0,00	0,06 ± 0,01
OATP6A1	ND	**0,31 ± 0,10**	0,03 ± 0,02	ND	0,03 ± 0,01	0,07 ± 0,02	ND	ND	ND	0,12 ± 0,00	0,05 ± 0,01

[a]mRNA expression level compared to reference gene (HPRT1); Maximum values are in bold; ND, transcripts were below the detection limit

Table 4

Expression levels of OATP mRNAs in ovarian cancer cell lines[a]

Protein name	OVCAR-3			SK-OV-3		
	RQ	**RQ-RQ_{Min}**	**RQ_{Max}-RQ**	**RQ**	**RQ-RQ_{Min}**	**RQ_{Max}-RQ**
OATP1A2	**1.00**	**0.1**	**0.06**	0.07	0.00	0.00
OATP1B1	ND	ND	ND	**1.00**	**0.01**	**0.01**
OATP1B3	1.00	0.00	0.00	**203.93**	**6.87**	**7.11**
OATP1C1	ND	ND	ND	ND	ND	ND
OATP2A1	**1.00**	**0.08**	**0.09**	0.45	0.04	0.05
OATP2B1	1.00	0.00	0.00	**70.57**	**0.99**	**1.01**
OATP3A1	1.00	**0.05**	**0.05**	0.18	0.00	0.00
OATP4A1	1.00	0.03	0.03	**6.29**	**0.05**	**0.05**
OATP4C1	**1.00**	**0.02**	**0.03**	0.07	0.00	0.00
OATP5A1	**1.00**	**0.00**	**0.00**	0.01	0.00	0.00
OATP6A1	ND	ND	ND	ND	ND	ND

[a]mRNA expression levels relative to OVCAR-3; Maximum values are in bold; ND, transcripts were below the detection limit

Table 5

Expression levels of ABC transporter mRNAs in ovarian cancer cell lines[a]

Protein name	OVCAR-3			SK-OV-3		
	RQ	**RQ-RQ_{Min}**	**RQ_{Max}-RQ**	**RQ**	**RQ-RQ_{Min}**	**RQ_{Max}-RQ**
MDR1	1.00	0.00	0.00	**1.73**	**0.02**	**0.02**
MRP2	1.00	0.01	0.01	**18.31**	**1.15**	**1.23**
MRP3	1.00	0.04	0.05	**5.30**	**0.28**	**0.29**
MRP7	1.00	0.01	0.02	0.93	0.00	0.00

[a]mRNA expression levels relative to OVCAR-3; Maximum values are in bold; ND, transcripts were below the detection limit

Fig. 1.

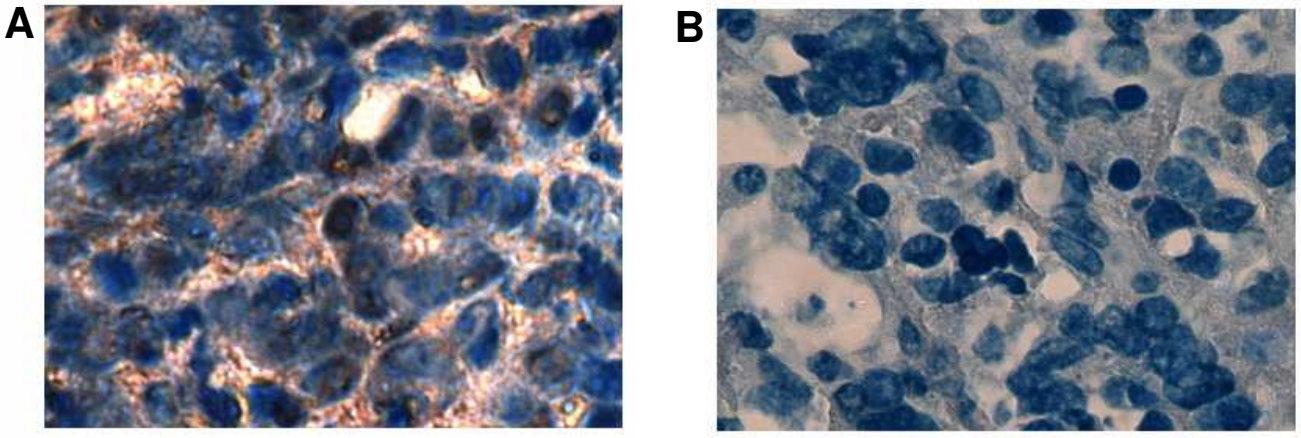

Fig. 2.

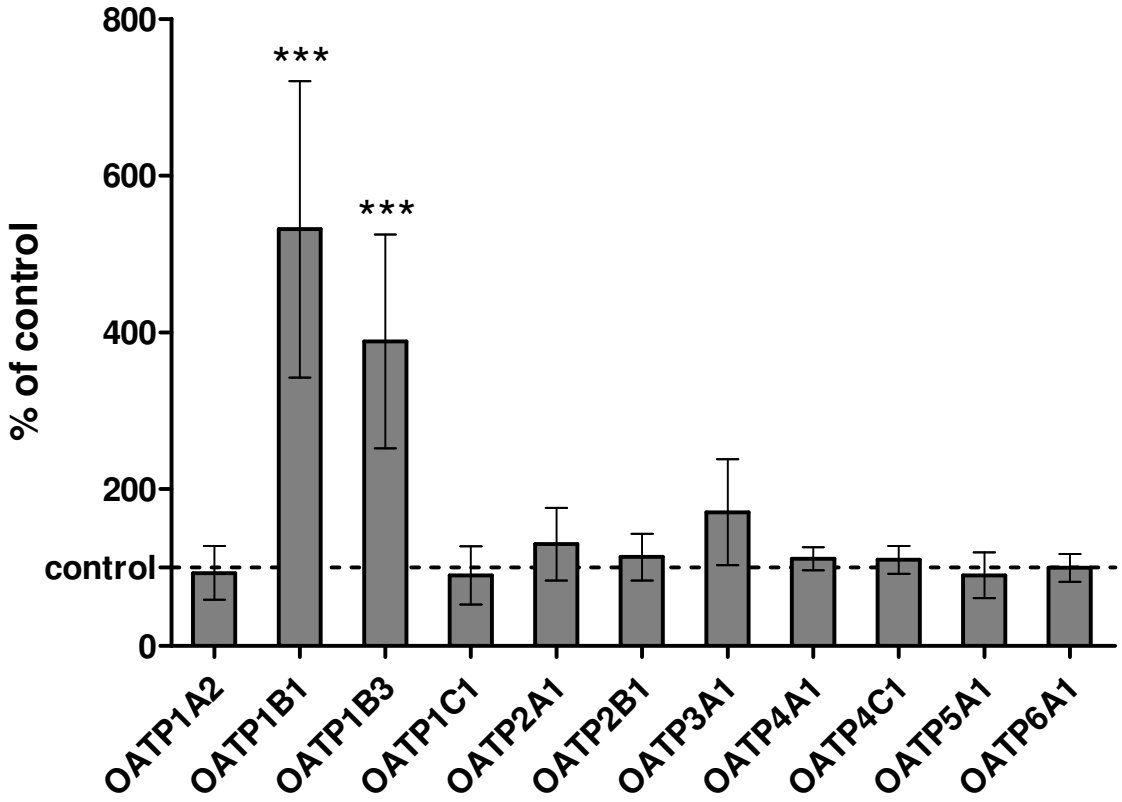
800
600
400
200
control
0
% of control
***
***
OATP1A2
OATP1B1
OATP1B3
OATP1C1
OATP2A1
OATP2B1
OATP3A1
OATP4A1
OATP4C1
OATP5A1
OATP6A1

Fig. 3

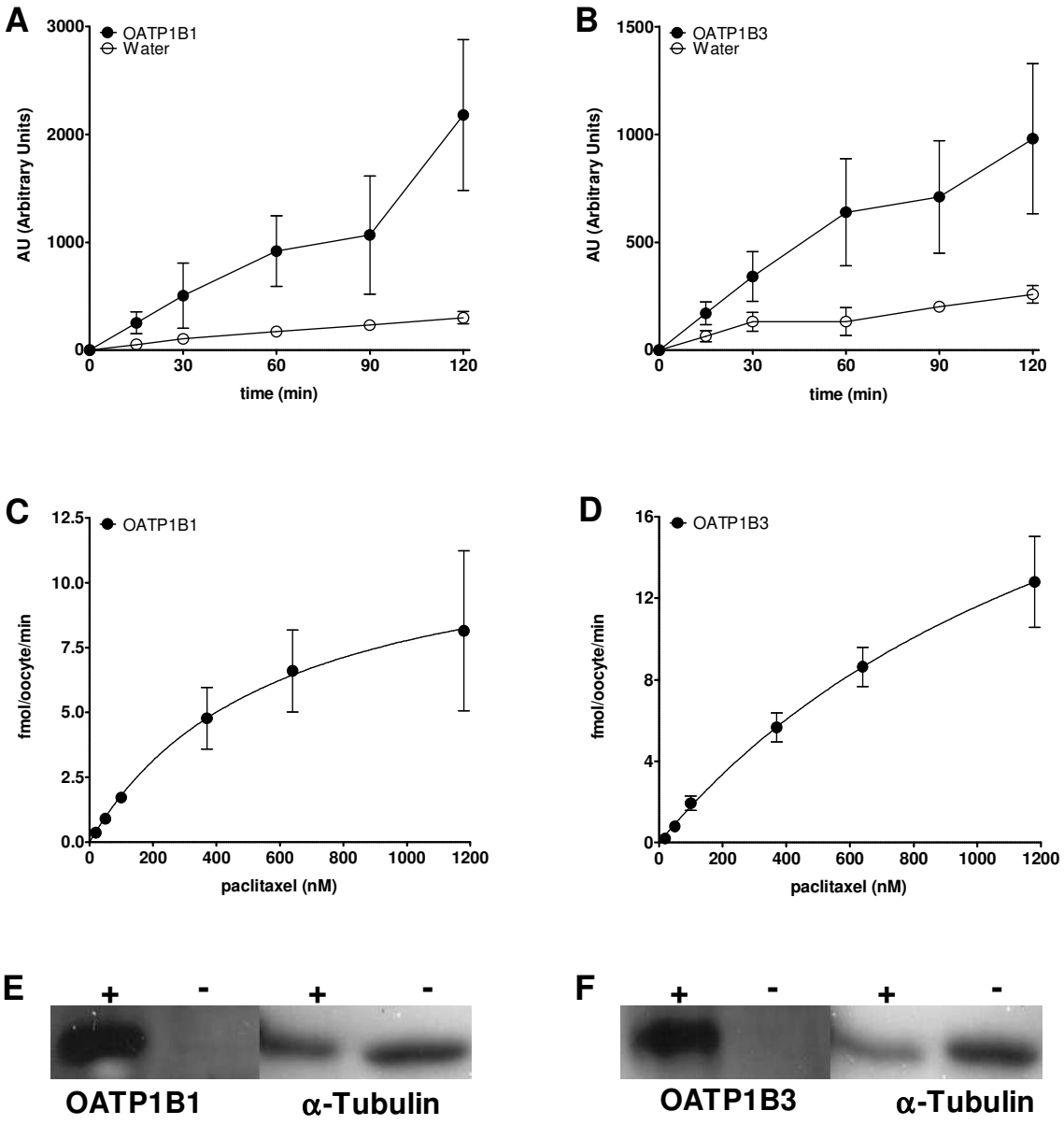
A
OATP1B1
Water
AU (Arbitrary Units)
time (min)
B
OATP1B3
Water
AU (Arbitrary Units)
time (min)
C
OATP1B1
fmol/oocyte/min
paclitaxel (nM)
D
OATP1B3
fmol/oocyte/min
paclitaxel (nM)
E
+ - + -
OATP1B1
α-Tubulin
F
+ - + -
OATP1B3
α-Tubulin

Fig. 4.

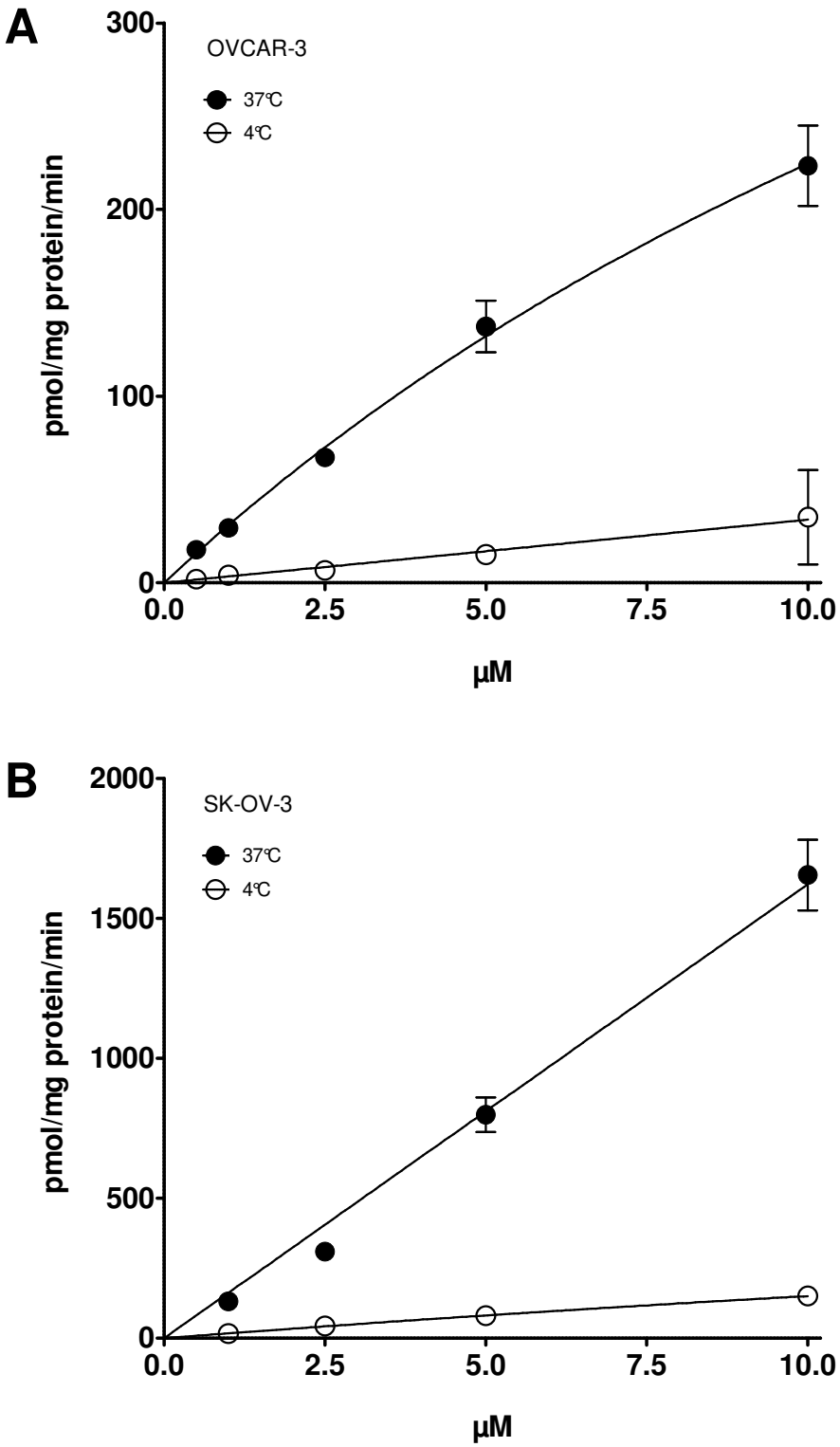
A
OVCAR-3
37℃
4℃
pmol/mg protein/min
300
200
100
0
0.0
2.5
5.0
7.5
10.0
μM
B
SK-OV-3
37℃
4℃
pmol/mg protein/min
2000
1500
1000
500
0
0.0
2.5
5.0
7.5
10.0
μM

Fig. 5.

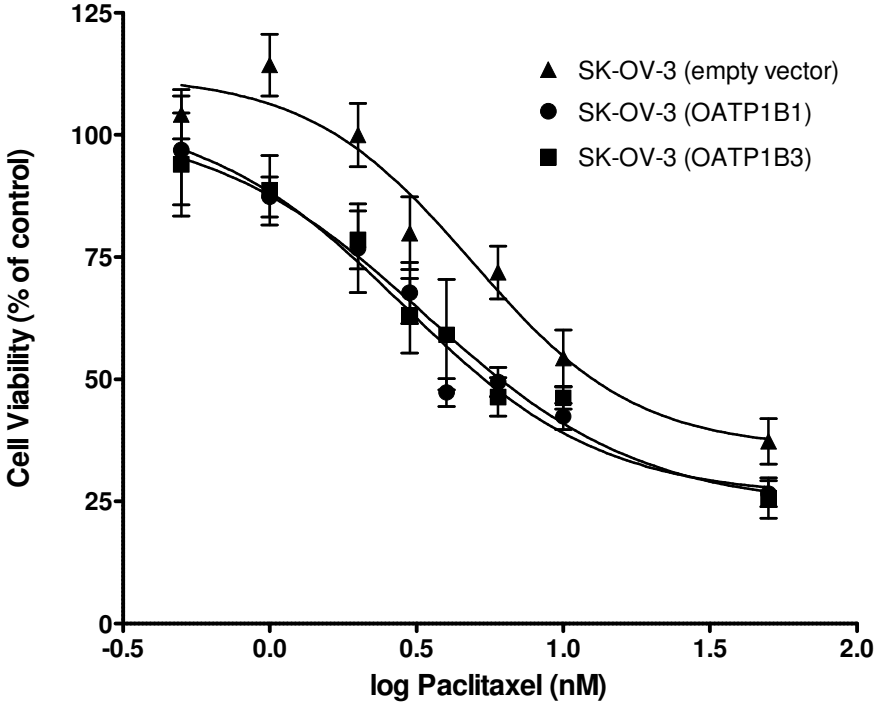
125
100
75
50
25
0
-0.5
0.0
0.5
1.0
1.5
2.0
Cell Viability (% of control)
log Paclitaxel (nM)
SK-OV-3 (empty vector)
SK-OV-3 (OATP1B1)
SK-OV-3 (OATP1B3)